

Multivariate Functional Linear Discriminant Analysis for the Classification of Short Time Series with Missing Data

Rahul Bordoloi¹, Clémence Réda¹, Orell Trautmann¹, Saptarshi Bej², and Olaf Wolkenhauer^{1,3,4,†}

¹Institute of Computer Science, University of Rostock, Germany

²Indian Institute of Science Education and Research, Thiruvananthapuram

³Leibniz–Institute for Food Systems Biology, Technical University of Munich, Freising, Germany

⁴Stellenbosch Institute of Advanced Studies (STIAS), South Africa

[†]Corresponding author: olaf.wolkenhauer@uni-rostock.de

Abstract

Functional linear discriminant analysis (FLDA) is a powerful tool that extends LDA–mediated multiclass classification and dimension reduction to univariate time–series functions. However, in the age of large multivariate and incomplete data, statistical dependencies between features must be estimated in a computationally tractable way, while also dealing with missing data. We here develop a multivariate version of FLDA (MUDRA) to tackle this issue and describe an efficient expectation/conditional–maximization (ECM) algorithm to infer its parameters. We assess its predictive power on the “Articulatory Word Recognition” data set and show its improvement over the state–of–the–art, especially in the case of missing data. MUDRA allows interpretable classification of data sets with large proportions of missing data, which will be particularly useful for medical or psychological data sets.

Keywords: time–series classification, linear discriminant analysis, missing data, functional data

1 Introduction

Linear discriminant analysis (LDA) is a popular strategy still widely used (Zhu et al., 2022; Mclaughlin and Su, 2023; Graf et al., 2024) for classification and dimensionality reduction. The origins trace back to Fisher’s discriminant (Fisher, 1936) and its multiclass extension (Rao, 1948). The main assumption of LDA is that samples of class $i = 1, 2, \dots, K$ follow a multivariate normal distribution of mean $\mu_i \in \mathbb{R}^d$ and shared covariance matrix $\Sigma \in \mathbb{R}^{d \times d}$ of full rank, denoted $\mathcal{N}_d(\mu_i, \Sigma)$. Then the Bayes optimal rule for classification is applied to predict the class $i(x)$ of a new sample $x \in \mathbb{R}^d$

$$i(x) \triangleq \arg \max_{i \in \{1, 2, \dots, K\}} \mathbb{P}(C = i | X = x), \quad (1)$$

$$\text{and} \quad \mathbb{P}(C = i | X = x) \propto \mathcal{N}_d(x; \mu_i, \Sigma) \pi_i \propto (\mu_i^\top \Sigma^{-1})x - \frac{1}{2} \mu_i^\top \Sigma \mu_i + \log \pi_i,$$

where $\pi_i \triangleq \mathbb{P}(C = i)$ is the prior probability of class i , by applying the Bayes theorem, reordering and ignoring terms that are constant across classes. This classification rule leads to a decision function linear in x . Parameters $(\mu_i)_{i \leq K}$, Σ , $(\pi_i)_{i \leq K}$ can be inferred by maximizing the joint likelihood on a set of training samples.

The advance of functional linear discriminant analysis (FLDA) (James and Hastie, 2001) allows us to handle cases where x is not simply a d –dimensional vector, but the output of a time–dependent multivariate function f associated with sample s : $x_s = f_s(t) \in \mathbb{R}^d$. Note that FLDA is restricted to the univariate case, i.e. when $d = 1$. In practice, one has of course no access to the true function $f_s : \mathbb{N}^* \rightarrow \mathbb{R}^d$, but only to some of its values $f_s(t_1^s), f_s(t_2^s), \dots, f_s(t_{n_s}^s)$ at a small number n_s of time points $t_1^s, t_2^s, \dots, t_{n_s}^s$. Such short time series appear in many practical scenarios.

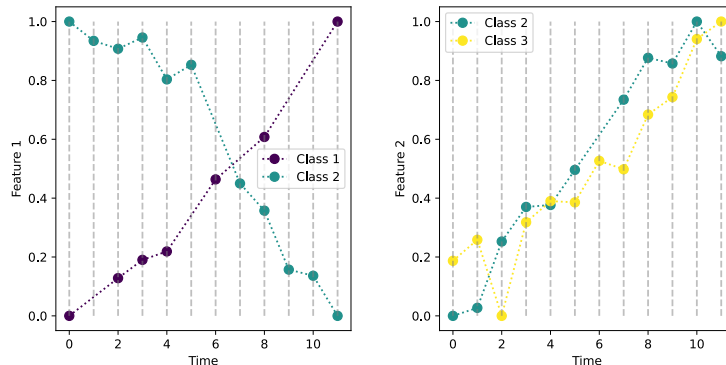


Figure 1: Example of a short multivariate time series with irregular sampling intervals and missing data. Each color corresponds to a class, and each plot represents a single feature. Some features or time points might be missing across individuals, for instance, Feature 2 is not measured for the individual in Class 1, and Feature 1 is not measured at the same time points between Class 1 and Class 2.

For instance, think of medical check-ups or psychological studies, where patients (individuals) from different conditions (classes) are surveyed for several variables (features) sparsely over weeks or months. Ignoring that those values come from the same function and simply concatenating values across all time points will lead to high-dimensional data strongly correlated across time points. This, in turn, would lead to numerical issues that prevent the estimation of the covariance matrix Σ .

Another challenge is that sampling occurs at irregular, short intervals of time points across samples (i.e. different, small values of n_s and different $(t_i^s)_i$ across samples s). Moreover, different sets of features might be measured in two distinct samples, meaning that even the value of d can vary across samples. Those challenges are exemplified in Figure 1. Notably, in this example, there is substantial missing data, such as Feature 2 in Class 1 and Feature 1 in Class 2, making traditional padding and imputation approaches impractical (Bier et al., 2022).

1.1 Related Work

In functional data analysis (Yao et al., 2005), time-series observations from sample s are considered as noisy samples from the underlying function f_s . This approach is particularly promising when one is interested in the overall shape of data. For example, for medical longitudinal data (Wang et al., 2022b) or data arising from psychological studies (Jebb et al., 2015), one is more interested in trends or the overall pattern of the entire cohort, rather than in individual fluctuations and noise sources. In many practical scenarios, the training data is collected from a large number of subjects at a small number of time points (Yoon et al., 2019). The grouping of subjects is based on a similarity of the curves or trends displayed. The learned model can then be used as a classifier to predict class membership for data from new subjects not in the training data set. In such cases, conventional LDA as shown in Equation 1 can't be directly applied, and time interval discretization is required.

James and Hastie (2001) addressed this issue by proposing a model which approximates observations as a noisy linear combination of spline curves, and applies a LDA-like inference procedure to the linear combination coefficients. However, this model only holds for univariate functional data. Applying FLDA individually to each curve is suboptimal due to the high dimension of data points and the fact that FLDA is not designed to estimate inter-feature correlations.

Multivariate time-series classification (TSC) methods have also been developed in the last decade, for instance, the autoregressive integrated moving average applied to multivariate data (marima) (Spliid, 2016). However, marima is only suitable for long-time series. The highest performing approaches for short TSC are today ensemble-of-classifiers methods, such as HIVE-COTE 1.0 (Lines et al., 2016) and 2.0 (Middlehurst et al., 2021), ROCKET (Dempster et al., 2020) and one of its most recent extension MultiRocket (Tan et al., 2022). HIVE-COTE algorithms combine the class probabilities returned by four different types of classifiers through a weighting step, which outputs the consensus probabilities, whereas ROCKET-like approaches apply a large number of data transformations using convolutional neural networks to create a massive amount of features. A linear classifier is then trained on those transformed features. Nonetheless, the ensemble architecture of HIVE-COTE and ROCKET might hinder the interpretability of the class probability outputs. Moreover, ROCKET-like methods require padding or imputation for handling missing data, which worsens the issue of high dimensional points and impedes interpretability again.

Statistical models tailored to multivariate functional data might overcome the issue of interpretability. Similarly to our work, Gardner-Lubbe (2021) presented an extension of FLDA to multivariate data. However, this approach completely ignores the issue of missing features. An alternative method proposed by Fukuda et al. (2023) involves the regularization of the underlying time-dependent functions, under the assumptions of regular sampling times and non-missing features. This thus proves impractical in our use case.

Finally, another line of research focuses on the growth mixture model (Ram and Grimm, 2009), which describes unobserved subpopulations as a noisy time-dependent linear combination of two latent variables. This approach is indeed adept at recognizing trends in longitudinal data, but the original model is also ill-equipped at handling missing data. The literature on the topic only partially solves this problem, as the issue of irregular sampling time points has been tackled in the prior works reviewed by Lee and Harring (2023). Even so, the proposed advancements cannot handle multiple, highly correlated and missing features.

1.2 Contributions

We introduce a multivariate functional linear discriminant analysis algorithm called MUDRA to tackle these issues. Our approach readily extends the scope of functional linear discriminant analysis described by James and Hastie (2001) to multivariate and missing data. MUDRA only requires that the set of features measured for a fixed sample s is the same across all the time points $t_1^s, t_2^s, \dots, t_{n_s}^s$. By approaching the problem from the purview of reduced rank regression, we were able to incorporate both time and feature-based irregularity without imputation. MUDRA generates a low-dimensional representation, based on the PARAFAC (Bro, 1997) tensor decomposition algorithm, that is particularly efficient for data sets with missing data and generates interpretable patterns. It can also reconstruct the mean time-dependent function across all samples from a class. We experimentally show the superior predictive power of MUDRA compared to baselines for time-series classification on a synthetic data set and on the ‘‘Articulatory Word Recognition’’ data set, in the presence of a large amount of missing data and when a low dimension is enough to capture the information from data. When there is a large amount of missing data, a common occurrence in real-life applications, MUDRA consistently outperforms ROCKET for low and high dimensionality.

1.3 Notation

If X is an $m \times n$ matrix, we will denote the rows and columns of X as $\mathbf{x}_{1,:}, \mathbf{x}_{2,:}, \dots, \mathbf{x}_{m,:}$ and $\mathbf{x}_{:,1}, \mathbf{x}_{:,2}, \dots, \mathbf{x}_{:,n}$ respectively. The ij^{th} element of X will be denoted by x_{ij} . If \mathbf{x}_t ’s are m -dimensional vectors, the i^{th} component of \mathbf{x}_t is denoted by $x_{t,i}$. The *column space* of X , which is the subspace spanned by $\{\mathbf{x}_1, \mathbf{x}_2, \dots, \mathbf{x}_n\}$ is denoted by $\mathcal{C}(X)$. A general pseudo-inverse of X is

denoted by X^- . Recall that if X is square and non-singular, the general pseudo-inverse is equal to the inverse: $X^- = X^{-1}$. We denote the identity matrix I regardless of its dimension.

For an $m \times n$ matrix X , $\text{vec}(X)$ denotes the *vectorization* of X as an mn dimensional vector, formed by stacking all of the columns of X sequentially, i.e.

$$\text{vec}(X) \triangleq [\mathbf{x}_{:,1}^\top \quad \mathbf{x}_{:,2}^\top \cdots \quad \mathbf{x}_{:,n}^\top]^\top.$$

The *Kronecker product* of two matrices $A_{m \times n}$ and $B_{p \times q}$ is an $mp \times nq$ matrix, defined by

$$A \otimes B \triangleq \begin{bmatrix} a_{11}B & a_{12}B & \cdots & a_{1n}B \\ a_{21}B & a_{22}B & \cdots & a_{2n}B \\ \vdots & \vdots & \ddots & \vdots \\ a_{m1}B & a_{m2}B & \cdots & a_{mn}B \end{bmatrix}.$$

We will use Kronecker products extensively to turn tensor computations into simpler matrix computations. A random $m \times n$ matrix X is said to follow a *matrix-variate normal distribution* (Nagar, 1999) with *mean* matrix $M_{m \times n}$, *row covariance* matrix $\Sigma_{m \times m}$ and *column covariance* matrix $\Psi_{n \times n}$, if $\text{vec}(X) \sim \mathcal{N}_{mn}(\text{vec}(M), \Psi \otimes \Sigma)$. It is denoted by $X \sim \mathcal{N}_{m \times n}(M, \Sigma, \Psi)$.

We will denote the variance-covariance matrix of a vector \mathbf{y} as $\mathbb{V}(\mathbf{y})$. For a matrix Σ , $\|\mathbf{y}\|_\Sigma$ will denote the *Mahalanobis norm* of \mathbf{y} with covariance Σ , defined as $\|\mathbf{y}\|_\Sigma^2 \triangleq \mathbf{y}^\top \Sigma^{-1} \mathbf{y}$. Similarly, for another vector \mathbf{x} , $\langle \mathbf{x}, \mathbf{y} \rangle_\Sigma$ will denote the *Mahalanobis inner product* with covariance Σ , defined as $\langle \mathbf{x}, \mathbf{y} \rangle_\Sigma \triangleq \mathbf{x}^\top \Sigma^{-1} \mathbf{y}$. The Mahalanobis inner product thus considers the correlation and variance between two vectors, which will be useful in finding linearly independent discriminants.

2 The MUDRA Algorithm

Formally, we introduce the available short multivariate time-series training data as follows. We consider a class \mathcal{C}_i of samples in which, for any sample j , F_{ij} features at T_{ij} time points have been measured: features $f_1^{ij}, f_2^{ij}, \dots, f_{F_{ij}}^{ij} \in \mathbb{N}^*$ at times $t_1^{ij}, t_2^{ij}, \dots, t_{T_{ij}}^{ij} \in \mathbb{N}^*$, for $i = 1, 2, \dots, K$ and $j \in \mathcal{C}_i$. The matrix of measurements of dimension $T_{ij} \times F_{ij}$ for sample j in class i is denoted Y_{ij} . The set of distinct features measured across all samples is denoted F , and the set of all sampling time points is T , that is

$$F \triangleq \bigcup_{i \leq K} \bigcup_{j \in \mathcal{C}_i} \bigcup_{k \leq F_{ij}} \{f_k^{ij}\} \quad \text{and} \quad T \triangleq \bigcup_{i \leq K} \bigcup_{j \in \mathcal{C}_i} \bigcup_{k \leq T_{ij}} \{t_k^{ij}\}.$$

Note that, since data is sampled irregularly, not all observations have been observed at some common time points or with common features. Thus, all matrices Y_{ij} will possibly have different dimensions. Finally, the number of samples in class i is $|\mathcal{C}_i| = m_i$.

In the remainder of this section, we describe a model that extends FLDA (James and Hastie, 2001) to multivariate functional data, that is, that models the observations as a noisy linear combination of spline functions which incorporates multiple features for the first time. Then, we propose an efficient parameter inference algorithm for this model and illustrate how to use it for classification and dimension reduction.

2.1 A Novel Multivariate Model for Time-Dependent Functional Observations

Similarly to the FLDA model introduced by James and Hastie (2001), we consider $b > 0$ B-spline functions of order 3 (Paul H. C. Eilers and Marx, 1996) denoted s_1, s_2, \dots, s_b to generate the space of functionals available to our model in a flexible fashion. Then for the multivariate observations associated with sample j in class \mathcal{C}_i , its spline matrix S_{ij} of dimensions $T_{ij} \times b$ is constructed by

evaluating the B-spline functions at each time point t_k^{ij}

$$S_{ij} \triangleq \begin{bmatrix} s_1(t_1^{ij}) & s_2(t_1^{ij}) & \cdots & s_b(t_1^{ij}) \\ s_1(t_2^{ij}) & s_2(t_2^{ij}) & \cdots & s_b(t_2^{ij}) \\ \vdots & \vdots & \ddots & \vdots \\ s_1(t_{T_{ij}}^{ij}) & s_2(t_{T_{ij}}^{ij}) & \cdots & s_b(t_{T_{ij}}^{ij}) \end{bmatrix} = \left(s_l(t_k^{ij}) \right)_{k \leq T_{ij}, l \leq b} . \quad (2)$$

We describe now how our model deviates from FLDA and integrates multiple features. Let C be the $F \times F$ identity matrix. Then, we truncate and reorder columns of C depending on the actual observed features for each sample. For sample $j \in \mathcal{C}_i$, define C_{ij} as the $F \times F_{ij}$ matrix formed by concatenating the $(f_1^{ij})^{\text{th}}, (f_2^{ij})^{\text{th}}, \dots, (f_{F_{ij}}^{ij})^{\text{th}}$ columns of C . We also introduce the spline coefficient matrix η_{ij} of dimensions $b \times F$. Similarly to the standard LDA model shown in Equation 1,

$$\eta_{ij} = \mu_i + \gamma_{ij} ,$$

where $\mu_i \in \mathbb{R}^{b \times F}$, $\gamma_{ij} \sim \mathcal{N}_{b \times F}(0, \Sigma, \Psi)$ is the autoregressive noise, and Σ and Ψ are both positive definite matrices. Finally, let ϵ_{ij} be the random matrix of measurement errors on sample $j \in \mathcal{C}_i$. We assume that it follows a matrix-variate normal distribution, i.e. $\epsilon_{ij} \sim \mathcal{N}_{T_{ij} \times F_{ij}}(0, \sigma^2 I, I)$ for some $\sigma > 0$. We then propose the following model of the multivariate time-dependent observations from sample j in class i

$$Y_{ij} = S_{ij}(\mu_i + \gamma_{ij})C_{ij} + \epsilon_{ij} .$$

We could leave our model at that, and go on inferring the values of parameters μ_i for $i = 1, 2, \dots, K$, σ , Σ , and Ψ . However, incorporating a reduced-rank regression into the model, by adding a supplementary rank constraint on the model parameters, leads to more interpretable models and easier dimension reduction (Izenman, 2008). Motivated by this reduced rank assumption, we fix the row rank r of our parameter space. Each class-specific mean parameter μ_i satisfies

$$\mu_i = \lambda_0 + \Lambda \alpha_i \xi ,$$

where λ_0 is the $b \times F$ matrix of spline coefficients for the population mean functional, the $(\alpha_i)_{i \leq K}$ are the class-specific reduced-rank spline coefficient matrices of dimensions $r \times r$, and $\Lambda \in \mathbb{R}^{b \times r}$ and $\xi \in \mathbb{R}^{r \times F}$ allow to reconstruct the full-rank spline coefficients for each class from the α_i 's. Thus, the final multivariate time-dependent model for $i = 1, 2, \dots, K$ and $j = 1, 2, \dots, m_i$ is

$$Y_{ij} = S_{ij}(\lambda_0 + \Lambda \alpha_i \xi + \gamma_{ij})C_{ij} + \epsilon_{ij} , \quad (3)$$

where $\epsilon_{ij} \sim \mathcal{N}_{T_{ij} \times F_{ij}}(0, \sigma^2 I, I)$, $\gamma_{ij} \sim \mathcal{N}_{b \times F}(0, \Sigma, \Psi)$, with parameters λ_0 , Λ , $(\alpha_i)_{i \leq K}$, ξ , σ , Σ , Ψ and hyperparameters b and r where $r \leq b$. Equation 3 handles fragmented curves, misaligned observation times, and accommodates measurement errors without imputation. The resulting decision function enables curve classification based on a representation of low dimension r . Class-specific characteristics are captured by the coefficients $(\alpha_i)_{i \leq K}$.

However, in this model, $\lambda_0, \Lambda, \alpha_i$ and ξ 's are interdependent, making parameter estimation harder. To solve this issue, we additionally enforce the following constraints:

$$\Lambda \text{ and } \xi^\top \text{ are orthogonal matrices, i.e. } \Lambda^\top \Lambda = I \quad \text{and} \quad \xi \xi^\top = I \quad \text{and} \quad \sum_{i=1}^K m_i \alpha_i = 0 . \quad (4)$$

Remark 1. Extension to FLDA. Equation 3 exactly retrieves FLDA when $F_{ij} = |F| = 1$ for all $i = 1, 2, \dots, K$ and $j \in \mathcal{C}_i$ (without the additional constraints in Equation 4). Indeed, in that case, $C = 1$, and the class i -specific coefficients become $\alpha_i \xi$.

Remark 2. Hyperparameters. *The selection of two hyperparameters, b (number of spline functions) and r (parameter rank), has a large impact on the quality of the approximation. We assess the model's performance on different values of r in the experimental study. For the selection of b , there is a tradeoff between the richness of the available space of functionals and the computation cost of the inference.*

2.2 An ECM Algorithm for Parameter Inference

As previously mentioned, fitting the model described in Equation 3 boils down to estimating parameters $\lambda_0, \Lambda, \alpha_i, \xi, \Sigma, \Psi$ and σ . We describe in Algorithm 1 an expectation/conditional-maximization (ECM) algorithm (Meng and Rubin, 1993) for parameter inference. The ECM algorithm is an extension to the well-known expectation/maximization (EM) algorithm for the iterative maximization of the joint log-likelihood on model parameters, which handles missing values in the E-step. This algorithm decouples the inference of most of the parameters across classes $i = 1, 2, \dots, K$ and samples $j \in \mathcal{C}_i$. If $\gamma_{ij} \sim \mathcal{N}_{b \times c}(0, \Sigma, \Psi)$ then thanks to the properties of matrix-variate normal distributions, $S_{ij}\gamma_{ij}C_{ij} \sim \mathcal{N}_{T_{ij} \times F_{ij}}(0, S_{ij}\Sigma S_{ij}^\top, C_{ij}^\top\Psi C_{ij})$. Let us then denote $\Sigma'_{ij} \triangleq S_{ij}\Sigma S_{ij}^\top$ and $\Psi'_{ij} \triangleq C_{ij}^\top\Psi C_{ij}$, which are assumed to be positive definite matrices. Therefore from Equation 3,

$$\text{vec}(Y_{ij}) \sim \mathcal{N}_{T_{ij}F_{ij}}(\text{vec}(S_{ij}(\lambda_0 + \Lambda\alpha_i\xi)C_{ij}), \sigma^2 I_{T_{ij}F_{ij}} + \Psi'_{ij} \otimes \Sigma'_{ij}). \quad (5)$$

In this case, the joint log-likelihood $\ell(\lambda_0, \Lambda, (\alpha_i)_i, \xi, \Sigma, \Psi, \sigma)$ on the parameters can be written as

$$\begin{aligned} & -\frac{1}{2} \sum_{i=1}^K \sum_{j=1}^{m_i} (\text{vec}(Y_{ij} - S_{ij}(\lambda_0 + \Lambda\alpha_i\xi)C_{ij})^\top (\sigma^2 I + \Psi'_{ij} \otimes \Sigma'_{ij})^{-1} \text{vec}(Y_{ij} - S_{ij}(\lambda_0 + \Lambda\alpha_i\xi)C_{ij}) \\ & + \log \det(\sigma^2 I + \Psi'_{ij} \otimes \Sigma'_{ij}) + T_{ij}F_{ij} \log(2\pi)). \end{aligned}$$

Algorithm 1 aims at maximizing $\ell(\lambda_0, \Lambda, (\alpha_i)_i, \xi, \Sigma, \Psi, \sigma)$ without computing any Kronecker product inverses to remain efficient. It relies on alternatively optimizing each parameter. Most prominently, this algorithm features the tensor decomposition algorithm PARAFAC (Bro, 1997) at Line 11. The Sylvester equation at Line 8 of Algorithm 1 is solved using the algorithm described in Bartels and Stewart (1972). The equation in Line 9 is solved by executing the generalized minimal residual (GMRES) method (Saad and Schultz, 1986). Further details are in Appendix A.

Remark 3. Theoretical Time Complexity. *MUDRA mainly focuses on reliability in the face of missing data for time-series classifications. However, ensuring a tractable algorithm for parameter inference is crucial. In each ECM iteration k , there is (1) $\sum_{i \leq K} m_i$ calls to the Bartels–Stewart algorithm (Line 8), (2) K calls to the GMRES algorithm (Line 9), (3) one call to the alternating least squares (ALS) minimization procedure for the PARAFAC tensor decomposition at Line 11, and finally, (4) an iterative optimization step at Lines 14 – 16.*

1. One call to the Bartels–Stewart algorithm on sample $j \in \mathcal{C}_i$ has an overall computational cost in $\mathcal{O}(T_{ij}^3 + F_{ij}^3 + T_{ij}F_{ij}^2 + T_{ij}^2F_{ij})$, by computing the Schur decompositions with the algorithm in Golub et al. (1979).
2. GMRES becomes increasingly expensive at each iteration: running k steps of the GMRES method has a time complexity in $\mathcal{O}(bFk^2)$. However, in theory, GMRES converges at step $k \leq b \times F$, so in the worst case, any call to GMRES has a time complexity in $\mathcal{O}(b^2F^2)$.
3. The PARAFAC decomposition is computed by alternatively minimizing on $w, \hat{\Lambda}, \hat{\xi}$ and c . The number of minimization steps across all parameters is limited to 100 in this function. Each single-parameter minimization is linear in this parameter, and then the time complexity is

Algorithm 1 MUDRA Algorithm: Model Parameter Inference

```

1: Input:  $Y_{ij}, S_{ij}, C_{ij}$  for  $i = 1, 2, \dots, K, j \in \mathcal{C}_i$ 
2: Hyperparameters:  $b \geq r, r \geq 1$ 
3: Initialize at random  $\lambda_0, \Lambda, \alpha_i, \xi, \Sigma, \Psi, \sigma$ 
4:  $Q_0 \leftarrow -\infty, k \leftarrow 1$ 
5:  $Q_k \leftarrow \ell(\lambda_0, \Lambda, (\alpha_i)_i, \xi, \Sigma, \Psi, \sigma)$  # joint log-likelihood  $\ell$ 
6: repeat
7:    $k \leftarrow k + 1$ 
8:   Solve the following equations in  $\hat{\gamma}'_{ij} \in \mathbb{R}^{T_{ij} \times F_{ij}}$  for  $i \leq K$  and  $j \in \mathcal{C}_i$ :
           
$$\sigma^2 (S_{ij} \Sigma S_{ij}^\top)^{-1} \hat{\gamma}'_{ij} + \hat{\gamma}'_{ij} C_{ij}^\top \Psi C_{ij} = (Y_{ij} - S_{ij}(\lambda_0 + \Lambda \alpha_i \xi) C_{ij}) C_{ij}^\top \Psi C_{ij}$$

9:   Solve the following equations in  $\hat{\beta}_i \in \mathbb{R}^{b \times F}$ :  $\sum_j S_{ij}^\top S_{ij} \hat{\beta}_i C_{ij} C_{ij}^\top = \sum_j S_{ij}^\top (Y_{ij} - \hat{\gamma}'_{ij}) C_{ij}^\top$ 
10:   $\hat{\lambda}_0 \leftarrow \sum_i \frac{m_i \hat{\beta}_i}{\sum_i m_i}, \beta'_i \leftarrow \hat{\beta}_i - \lambda_0, \beta \leftarrow [\beta'_i, i = 1, 2, \dots, K] \in \mathbb{R}^{b \times F \times K}$ 
11:  Find a  $r$ -way canonical decomposition  $(w, \hat{\Lambda}, \hat{\xi}, \mathbf{c})$ :  $\beta \approx \sum_{u=1}^r w_u (\hat{\Lambda}_{:,u} \otimes \hat{\xi}_{u,:}^\top \otimes \mathbf{c}_{u,:})$ 
12:   $\hat{\alpha}_i \leftarrow \sum_{u=1}^r w_u \mathbf{c}_{i,u}$  and  $\hat{\gamma}'_{ij} \leftarrow (S_{ij}^\top S_{ij})^{-1} S_{ij}^\top \hat{\gamma}'_{ij} C_{ij}^\top (C_{ij} C_{ij}^\top)^{-1}$ 
13:   $\hat{\Sigma} \leftarrow I_b, \hat{\Psi} \leftarrow I_F, \hat{\sigma} \leftarrow 1$ 
14:  while  $\hat{\Sigma}, \hat{\Psi}$  and  $\hat{\sigma}$  do not converge do
15:     $\hat{\Sigma} \leftarrow (\sum_{i,j} F_{ij})^{-1} \sum_{i,j} \hat{\gamma}'_{ij} \hat{\Psi}^{-1} \hat{\gamma}'_{ij}^\top$  and  $\hat{\Psi} \leftarrow (\sum_{i,j} T_{ij})^{-1} \sum_{i,j} \hat{\gamma}'_{ij}^\top \hat{\Sigma}^{-1} \hat{\gamma}'_{ij}$ 
16:     $\hat{\sigma}^2 \leftarrow (\sum_{i,j} T_{ij} F_{ij})^{-1} \sum_{i,j} \|Y_{ij} - S_{ij}(\hat{\lambda}_0 + \hat{\Lambda} \hat{\alpha}_i) C_{ij} - \hat{\gamma}'_{ij}\|_F^2 + \text{tr}\{C_{ij}^\top \hat{\Psi} C_{ij}\} \text{tr}\{S_{ij} \hat{\Sigma} S_{ij}^\top\}$ 
17:  end while
18:   $Q_k \leftarrow \ell(\hat{\lambda}_0, \hat{\Lambda}, (\hat{\alpha}_i)_i, \hat{\xi}, \hat{\Sigma}, \hat{\Psi}, \hat{\sigma})$  # joint log-likelihood  $\ell$  on estimated parameters
19:  if  $Q_{k-1} < Q_k$  then
20:     $\lambda_0 \leftarrow \hat{\lambda}_0, \Lambda \leftarrow \hat{\Lambda}, (\alpha_i)_i \leftarrow (\hat{\alpha}_i)_i, \xi \leftarrow \hat{\xi}, \Sigma \leftarrow \hat{\Sigma}, \Psi \leftarrow \hat{\Psi}, \sigma \leftarrow \hat{\sigma}$ 
21:  end if
22: until  $Q_{k-1} \geq Q_k$ 
23: return  $\lambda_0, \Lambda, (\alpha_i)_i, \xi, \Sigma, \Psi, \sigma$ 

```

mainly driven by the matrix inversion and product operations.

4. Theoretically, the iterative optimization step in Lines 14 – 16 converges, but no convergence rate is provided. In practice, we chose to change the criteria to either stay under a maximum number of iterations (50 in our experiments) or until the value of $\hat{\sigma}$ has converged: at step q of the iteration, $|\hat{\sigma}_{q-1}^{-1}(\hat{\sigma}_{q-1} - \hat{\sigma}_q)| < 10^{-5}$. Then, the remaining cost of this step mainly stems from the matrix products.

We also compare the empirical runtimes of MUDRA and one algorithm from the state-of-the-art, ROCKET (Dempster et al., 2020) in the experimental study in Section 3.

Remark 4. Implementation. In our implementation of MUDRA, we resort to the Bartels–Stewart algorithm and GMRES present in the Python package `scipy` (Virtanen et al., 2020). Moreover, we consider the PARAFAC decomposition function in Python package `Tensorly` (Kossaifi et al., 2016).

2.3 Classification and Dimension Reduction with MUDRA

Once the parameter values in Equation 3 have been inferred by running Algorithm 1, a LDA-like approach to classification (see Equation 1) can be applied to a new sample $Y \in \mathbb{R}^{T' \times F'}$. Our model allows to define the density function f_i of class $i = 1, 2, \dots, K$ and the prior probability π_i . In our experiments, we assume a uniform prior, that is, $\pi_i = 1/K$ for all $i = 1, 2, \dots, K$, but other types of

prior might also be considered. Then, the class predicted for sample Y is

$$i(Y) \triangleq \arg \max_{i \in \{1, 2, \dots, K\}} \log \mathbb{P}(C = i | X = Y) \propto \log f_i(Y) + \log \pi_i. \quad (6)$$

Let us derive the expression of f_i from Equation 5. Let us denote S_Y the spline matrix in Equation 2 associated with time points in Y , C_Y the corresponding matrix of reordered feature columns, $M_Y \triangleq \sigma^2 I + (C_Y^\top \Psi C_Y) \otimes (S_Y \Sigma S_Y^\top)$ and

$$\text{vec}(\hat{\alpha}_Y) \triangleq ((\xi C_Y \otimes \Lambda^\top S_Y^\top) M_Y^{-1} (C_Y^\top \xi^\top \otimes S_Y \Lambda))^{-\frac{1}{2}} (\xi C_Y \otimes \Lambda^\top S_Y^\top) M_Y^{-1} \text{vec}(Y - S_Y \lambda_0 C_Y).$$

Then, ignoring constant factors in i and leveraging the computations made in Appendix B, $\log f_i(Y)$ in Equation 6 can be replaced with

$$\begin{aligned} \log f_i(Y) &= -\frac{1}{2} \|\text{vec}(Y - S_Y(\lambda_0 + \Lambda \alpha_i \xi) C_Y)\|_{M_Y}^2 + \log \det(M_Y) + T_Y F_Y \log(2\pi) \\ &\propto -\frac{1}{2} \|\text{vec}(Y - S_Y(\lambda_0 + \Lambda \alpha_i \xi) C_Y)\|_{M_Y}^2 \\ &\propto -\frac{1}{2} \|\text{vec}(\hat{\alpha}_Y) - ((\xi C_Y \otimes \Lambda^\top S_Y^\top) M_Y^{-1} (C_Y^\top \xi^\top \otimes S_Y \Lambda))^{-\frac{1}{2}} \text{vec}(\alpha_i)\|. \end{aligned}$$

Moreover, Equation 14 in Appendix B shows that the covariance of $\hat{\alpha}_Y$, $\mathbb{V}[\text{vec}(\hat{\alpha}_Y)] = I$. $\hat{\alpha}_Y$ can be reshaped into an $r \times r$ matrix. Then, we obtain an r^2 -dimensional representation of Y .

3 Experimental Study

We describe the empirical results of MUDRA in this section regarding predictive power, interpretability, and time efficiency.

3.1 Time-Series Classification on a Synthetic Data set

We built a data set with two features, 12 time points, two classes, and 300 samples as described in Appendix C. For this experiment, we set $b = 7$ spline basis functions as a tradeoff between performance and computational cost.

To assess the predictive power of our model, we collected the mean squared error (MSE) values between each estimated functional point and its ground truth, and the F_1 scores for the corresponding classification task for multiple values of r . MSE values and F_1 scores are reported in respectively Figure 3a and Figure 3b. As expected, in Figure 3a, MSE decreases when r , that is, the representation rank, increases. Interestingly, MSE seems to increase again from $r = 2$, which we interpret as being due to overfitting. Figure 3b shows that for $r > 1$, the F1-score for classification is almost 100%. Thus, the optimal value for this data set that balances between performance and speed is $r = 2$. Figure 2 compares the true functionals from the synthetic data set and those inferred using MUDRA with hyperparameter $r = 3$.

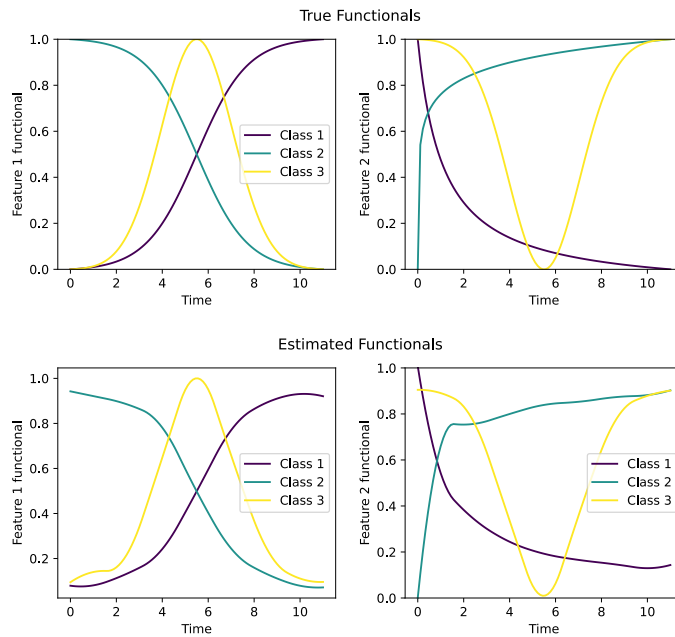


Figure 2: Top plot: curves of feature 1 (on the left) and feature 2 (right) across the three classes. Bottom plot: corresponding estimated curves by MUDRA with $r = 3$, $b = 7$.

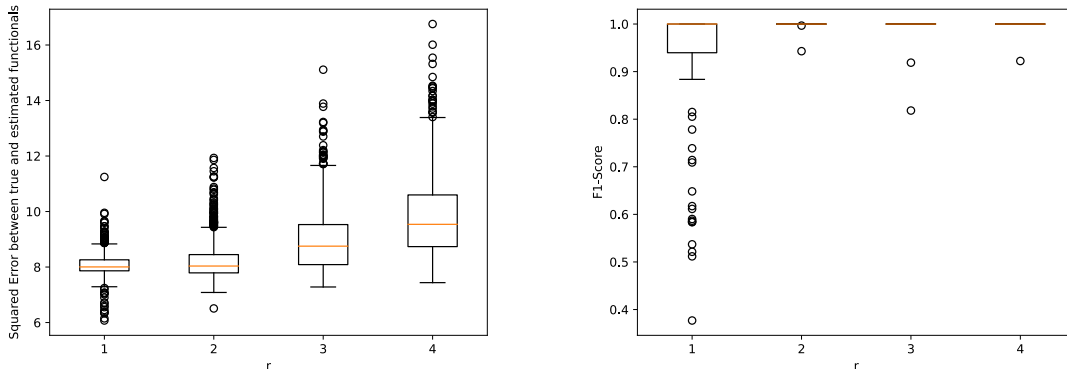
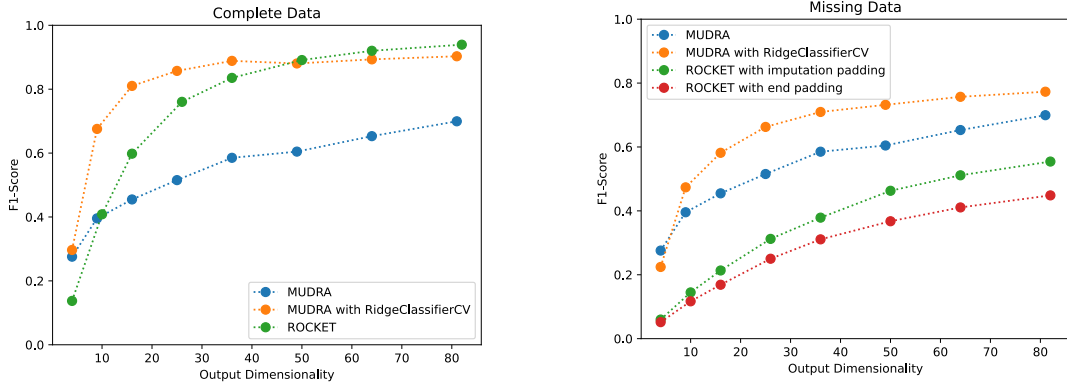


Figure 3: Synthetic experiments with $b = 7$. Left: MSE between estimated and true functional points for $r \in \{1, 2, 3, 4\}$. Right: F_1 -scores on the classification task on the synthetic data set for $r \in \{1, 2, 3, 4\}$.

3.2 Time-Series Dimension Reduction on a Benchmark Data set

We also applied the MUDRA algorithm to the real-world data set ‘‘Articulatory Word Recognition’’ from Dau et al. (2019). Further details about the simulation of missing data are present in Appendix C. A recent review by Ruiz et al. (2021) showed that ROCKET (Dempster et al., 2020) is currently the best-performing model, both in terms of efficiency and accuracy, for feature transfor-



(a) MUDRA versus ROCKET on complete data. The blue curve correspond to the Bayes-optimal rule in MUDRA, the orange one is the dimension reduction in MUDRA combined with a ridge regression classifier, the green curve correspond to ROCKET-transformed features fed to the classifier.

(b) MUDRA versus ROCKET on missing data. The blue curve correspond to the Bayes-optimal rule in MUDRA, the orange one is the dimension reduction in MUDRA combined with a ridge regression classifier, the green (resp., red) curve correspond to ROCKET-transformed features with “imputation” (resp., “end”)-type padding fed to the classifier.

Figure 4: ROCKET versus MUDRA with a ridge regression-based classifier on the “Articulatory Word Recognition” data set with $b = 9$ and for $r \in [1, 9]$.

mation in short-time-series classification. We applied MUDRA or ROCKET to perform a dimension reduction on the data set. Resulting features were fed to a ridge regression-based classifier. Such a procedure allows to test how informative the resulting representations are, which is a first step towards interpretability. We also classified the data directly through the Bayes-optimal classifier described in Section 2.3. Since ROCKET always reduces to an even number of dimensions, and MUDRA to r^2 dimensions, to ensure fairness when comparing both algorithms, we considered for ROCKET the smallest even number which was larger than r^2 . The two plots in Figure 4 report the F_1 scores obtained for the classification tasks for multiple values of output dimension r on complete data (i.e. without any missing data) and on missing data, where the procedure in Appendix C has been applied to the data set. Figure 4a shows that MUDRA competes with ROCKET for very low-dimensional representations, but ROCKET overtakes MUDRA as we increase the output dimension. However, when data is missing, ROCKET cannot be applied directly. Inspired by Bier et al. (2022), we employed two forms of padding to the data set prior to running ROCKET:

1. **“Imputation”-type:** The recorded data points are aligned according to their sampling times. Missing time points and missing features are denoted with 0.
2. **“End”-type:** All missing features are imputed with 0. All measured time points are concatenated. 0s are appended at the end to obtain time series of the same length.

Figure 4b shows that MUDRA clearly outperforms ROCKET in both of these cases.

3.3 Empirical Runtime of the MUDRA Algorithm

To assess the empirical time complexity of MUDRA, we collected the runtimes over $N = 1,000$ iterations of both MUDRA and ROCKET combined with a ridge classifier on the real-life data set (without missing data, $r = 7$, $b = 9$). Resulting runtimes are reported in Figure 5.

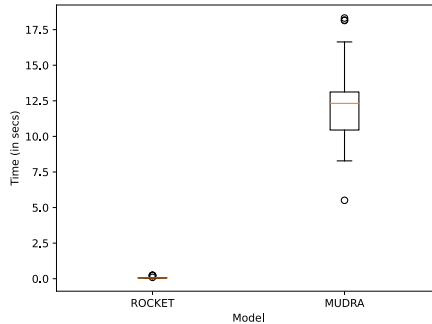


Figure 5: Runtimes for ROCKET and MUDRA on the complete real-life data set for $r = 7$ and $b = 9$ ($N = 1,000$ iterations per algorithm).

As evidenced by Figure 5, the current implementation of MUDRA is approximately 12 times slower in average than ROCKET. Since ROCKET is a simple algorithm that shifts most of the burden of inference to the subsequent classification algorithm, it is extremely fast. However, as previously mentioned, it lacks some of the predictive power of MUDRA.

4 Conclusion

This work presents a novel approach to dealing with missing data in multivariate functional data, which has historically proven to be a challenging problem for short-time-series classification. Contemporary algorithms, which achieve optimal performance, typically resort to padding; however, this strategy proves suboptimal for very short time series with a large proportion of missing data. Our proposed algorithm, MUDRA, uniquely enables model training on selective fragments of a high-dimensional surface without necessitating regularization to reconstruct the entire surface for each sample. This eliminates the need for padding and imputation. Our algorithm outperforms the current state-of-the-art models in the cases where a very low-dimensional representation is required and/or a large proportion of the data is missing. Such cases frequently arise in real-life data, especially in biomedical applications.

While our approach demonstrates considerable flexibility and efficiency, it has shortcomings. Empirically, we show that the MUDRA algorithm sacrifices some time efficiency in favor of interpretability. Improving on the implementation of Algorithm 1 by resorting to faster routines (Nguyen et al., 2016; Song et al., 2022), switching the programming language to C and Fortran, or approximating solution equations (Wang et al., 2022a) could tackle this issue.

On the theoretical side, one issue we could not solve was irregularly sampled features for one subject. Consider data being recorded for a sample Y_{ij} at time points t_1^{ij} and t_2^{ij} . If the features recorded for Y_{ij} at t_1^{ij} are not the same as at t_2^{ij} , our model cannot train on that datapoint without resorting to the imputation or deletion of some of the features. Another significant limitation is the assumption of common covariance matrices Σ and Ψ for the auto-regressive noise in each class, which stem from the LDA standpoint. This is sometimes not representative of real data, for example, clinical data, as certain conditions can have a major impact on the variability of levels of certain metabolites. A quadratic discriminant analysis (QDA) approach might have mitigated these issues. However, class-specific covariance matrices raise a number of computational problems in the ECM algorithm and do not lead to the relatively simple expression for the dimension reduction of a new sample. Tackling these shortcomings would improve the application of short-time-series classification algorithms to real-life use cases.

Acknowledgments and Disclosure of Funding

C.R. has received funding from the European Union’s HORIZON 2020 Programme under grant agreement no. 101102016 (RECeSS, HORIZON MSCA Postdoctoral Fellowships–European Fellowships). O.W. acknowledges support from the German Research Foundation (DFG) FK515800538 (learning convex data spaces).

Conflicts of Interest

The authors declare that no conflicts of interest were associated with this work.

Code Availability

The source code for MUDRA (Algorithm 1), along with documentation, is available at the following GitHub repository: <https://github.com/rbordoloi/MUDRA> under a GPL–3 license.

Appendix A. The ECM Algorithm

To guarantee convergence, we assume that $S_{ij}\Sigma S_{ij}^\top$ and $C_{ij}^\top\Psi C_{ij}$ are invertible for each i and j . Our objective is to maximize

$$Q = -\frac{1}{2} \sum_{i,j} \left(\frac{1}{\sigma^2} \|Y_{ij} - S_{ij}(\lambda_0 + \Lambda\alpha_i\xi + \gamma_{ij})C_{ij}\|_F^2 + T_{ij}F_{ij} \log \sigma^2 + \text{tr}\{\Psi^{-1}\gamma_{ij}^\top\Sigma^{-1}\gamma'_{ij}\} \right. \\ \left. + T_{ij} \log \det(\Psi) + F_{ij} \log \det(\Sigma) \right).$$

A.1 The E-Step

To simplify calculations, we will drop all indices and look at only one data point from one class, as the aggregate can be calculated by doing similar calculations for all data points and computing the arithmetic mean at the end. Thus the simplified model can be written as

$$Y = S(\beta + \gamma)C + \epsilon,$$

where S and C are $T \times b$ and $n \times F$ matrices respectively. The idea is to compute the expectation of $S\gamma C = \gamma'$ instead of γ itself like in James and Hastie (2001) and write Q in terms of γ' . This will allow us to simplify and use Bartels and Stewart (1972) to find the expectation without computing any tensor products. The log-likelihoods, ignoring proportionality constants, are as follows.

$$l(Y) = -\text{vec}(Y - S\beta)^\top (\sigma^2 I \otimes I + \Psi \otimes \Sigma)^{-1} \text{vec}(Y - S\beta C) - \log(|\sigma^2 I \otimes I + \Psi \otimes \Sigma|) \\ l(Y, \gamma') = -\frac{\text{vec}(Y - S\beta C - \gamma')^\top \text{vec}(Y - S\beta C - \gamma')}{\sigma^2} - \text{vec}(\gamma')^\top ((C^\top \Psi C) \otimes (S\Sigma S^\top))^{-1} \text{vec}(\gamma') \\ - TF \log(\sigma^2) - F \log \det(S\Sigma S^\top) - T \log \det(C^\top \Psi C) \\ = -\frac{1}{\sigma^2} \|Y - S\beta C - \gamma'\|_F^2 - (C^\top \Psi C)^{-1} \gamma'^\top (S\Sigma S^\top) \gamma' - TF \log(\sigma^2) \\ - T \log \det(C^\top \Psi C) - F \log \det(S\Sigma S^\top).$$

This is because $\gamma \sim \mathcal{N}_{b \times n}(0, \Sigma, \Psi) \implies \gamma' = S\gamma \sim \mathcal{N}_{m \times n}(0, S\Sigma S^\top, C^\top \Psi C)$ by Theorem 2.3.10 in Nagar (1999). Let us set $\Sigma' = S\Sigma S^\top$ and $\Psi' = C^\top \Psi C$. We know that $\mathbb{E}[\gamma'|Y = y] = \int \gamma' \frac{f_{Y, \gamma'}(y, \gamma')}{f_Y(y)} d\gamma'$, for all $y : f_Y(y) > 0$. Let us ignore all terms not depending on γ' . We will work with the terms in the exponential depending on γ' in log space to avoid numerical instability.

$$\frac{1}{\sigma^2} (\text{vec}(Y - S\beta C)^\top \text{vec}(\gamma') + \text{vec}(\gamma')^\top \text{vec}(Y - S\beta C) - \text{vec}(\gamma')^\top \text{vec}(\gamma')) \\ - \text{vec}(\gamma')^\top (\Psi' \otimes \Sigma')^{-1} \text{vec}(\gamma') \\ = \frac{1}{\sigma^2} (\text{vec}(Y - S\beta C)^\top \text{vec}(\gamma') + \text{vec}(\gamma')^\top \text{vec}(Y - S\beta C) \\ - \text{vec}(\gamma')^\top (I + \sigma^2 (\Psi' \otimes \Sigma')^{-1}) \text{vec}(\gamma')).$$

Let $M = (I + \sigma^2 (\Psi' \otimes \Sigma')^{-1})$. Clearly, M is symmetric. Then by completing the square inside the term multiplied by $-\frac{1}{\sigma^2}$ we have

$$- \text{vec}(Y - S\beta C)^\top M^{-1} \text{vec}(Y - S\beta C) + \text{vec}(Y - S\beta C)^\top M^{-1} \text{vec}(Y - S\beta C) \\ - \text{vec}(Y - S\beta C)^\top M^{-\frac{1}{2}} M^{\frac{1}{2}} \text{vec}(\gamma') - \text{vec}(\gamma')^\top M^{\frac{1}{2}} M^{-\frac{1}{2}} \text{vec}(Y - S\beta C) + \text{vec}(\gamma')^\top M \text{vec}(\gamma') \\ = -\text{vec}(Y - S\beta C)^\top M^{-1} \text{vec}(Y - S\beta C) \\ + (M^{\frac{1}{2}} \text{vec}(\gamma') - M^{-\frac{1}{2}} \text{vec}(Y - S\beta C))^\top (M^{\frac{1}{2}} \text{vec}(\gamma') - M^{-\frac{1}{2}} \text{vec}(Y - S\beta C)) \\ = -\text{vec}(Y - S\beta C)^\top M^{-1} \text{vec}(Y - S\beta C) \\ + (\text{vec}(\gamma') - M^{-1} \text{vec}(Y - S\beta C))^\top M (\text{vec}(\gamma') - M^{-1} \text{vec}(Y - S\beta C)).$$

Clearly, $\text{vec}(\gamma')|Y \sim N(M^{-1}\text{vec}(Y - S\beta C), \sigma^2 M^{-1})$. So

$$\begin{aligned}
 \mathbb{E}[\text{vec}(\gamma')|Y] &= M^{-1}\text{vec}(Y - S\beta C) \\
 \implies \mathbb{E}[\text{vec}(\gamma')|Y] &= (I \otimes I + \sigma^2(\Psi' \otimes \Sigma')^{-1})^{-1}\text{vec}(Y - S\beta C) \\
 &= (I \otimes I + (\Psi'^{-1} \otimes I)(I \otimes \sigma^2 \Sigma'^{-1}))^{-1}\text{vec}(Y - S\beta C) \\
 &= ((\Psi'^{-1} \otimes I)(\Psi' \otimes I) + (\Psi'^{-1} \otimes I)(I \otimes \sigma^2 \Sigma'^{-1}))^{-1}\text{vec}(Y - S\beta C) \\
 &= (\Psi' \otimes I + I \otimes \sigma^2 \Sigma'^{-1})^{-1}(\Psi' \otimes I)\text{vec}(Y - S\beta C) \\
 &= (\Psi' \otimes I + I \otimes \sigma^2 \Sigma'^{-1})^{-1}\text{vec}((Y - S\beta C)\Psi'^{\top}) .
 \end{aligned}$$

Now, we can find $(\Psi' \otimes I + I \otimes \sigma^2 \Sigma'^{-1})^{-1}\text{vec}((Y - S\beta)\Psi'^{\top})$ by solving the Sylvester equations $\sigma^2(\Sigma'^{-1})X + X\Psi'^{\top} = (Y - S\beta)\Psi'^{\top}$ using the Bartels and Stewart (1972) algorithm. Let this value be called $\mu_{\gamma'}$. Also, let $\mu_{\gamma} = \mathbb{E}[\gamma|Y]$ and $Y' = Y - S\beta C$. From Nagar (1999) we know that is $X \sim \mathcal{N}_{m \times n}(\mu, \Sigma, \Psi)$, $\mathbb{E}[X^{\top}AX] = \text{tr}\{\Sigma A^{\top}\}\Psi + \mu^{\top}A\mu$

$$\begin{aligned}
 \mathbb{E}[\|Y' - S\gamma C\|_F^2] &= \text{tr}\{\mathbb{E}[(Y' - S\gamma C)^{\top}(Y' - S\gamma C)]\} \\
 &= \text{tr}\{\mathbb{E}[Y'^{\top}Y' + C^{\top}\gamma^{\top}S^{\top}S\gamma C - Y'^{\top}S\gamma C - C^{\top}\gamma^{\top}S^{\top}Y']\} \\
 &= \text{tr}\{Y'^{\top}Y'\} - 2\text{tr}\{Y'^{\top}S\mu_{\gamma}C\} + \text{tr}\{C^{\top}\mathbb{E}[\gamma^{\top}S^{\top}S\gamma]C\} \\
 &= \text{tr}\{Y'^{\top}Y'\} - 2\text{tr}\{Y'^{\top}S\mu_{\gamma}C\} + \text{tr}\{C^{\top}(\text{tr}\{\Sigma S^{\top}S\}\Psi + \mu_{\gamma}S^{\top}S\mu_{\gamma})C\} \\
 &= \text{tr}\{Y'^{\top}Y'\} - 2\text{tr}\{Y'^{\top}S\mu_{\gamma}C\} \\
 &\quad + \text{tr}\{C^{\top}\text{tr}\{\Sigma S^{\top}S\}\Psi C\} + \text{tr}\{C^{\top}\mu_{\gamma}S^{\top}S\mu_{\gamma}C\} \\
 &= \text{tr}\{Y'^{\top}Y'\} - 2\text{tr}\{Y'^{\top}\mu_{\gamma'}\} + \text{tr}\{C^{\top}\Psi C\}\text{tr}\{S\Sigma S^{\top}\} + \text{tr}\{\mu_{\gamma'}^{\top}\mu_{\gamma'}\} \\
 \implies \mathbb{E}\left[\sum_{i,j} \|Y'_{ij} - S_{ij}\gamma_{ij}C_{ij}\|_F^2\right] &= \sum_{i,j} \left(\|Y_{ij} - S_{ij}(\lambda_0 + \Lambda\alpha_i\xi)C_{ij} - \mu_{\gamma'_{ij}}\|_F^2 + \text{tr}\{C_{ij}^{\top}\Psi C_{ij}\}\text{tr}\{S_{ij}\Sigma S_{ij}^{\top}\} \right) .
 \end{aligned}$$

With some abuse of notation, we will call $\hat{\mu}_{\gamma'_{ij}}$ as γ'_{ij} .

A.2 The CM-Step

Since many of the parameters are interdependent, we will use conditional maximization. For a parameter p , \hat{p} denotes the estimate at the next step. For convenience we will call $\mu_{\gamma'_{ij}}$ as γ'_{ij} . Our objective is to maximize

$$\begin{aligned}
 Q &= -\frac{1}{2} \sum_{i,j} \left(\frac{1}{\sigma^2} (\|Y_{ij} - S_{ij}(\lambda_0 + \Lambda\alpha_i\xi)C_{ij} - \gamma'_{ij}\|_F^2 + \text{tr}\{C_{ij}^{\top}\Psi C_{ij}\}\text{tr}\{S_{ij}\Sigma S_{ij}^{\top}\}) + T_{ij}F_{ij} \log \sigma^2 \right. \\
 &\quad \left. + \text{tr}\{\Psi^{-1}\gamma_{ij}^{\top}\Sigma^{-1}\gamma_{ij}\} + T_{ij} \log \det(\Psi) + F_{ij} \log \det(\Sigma) \right) ,
 \end{aligned}$$

where $\|\cdot\|_F$ denotes the Frobenius norm.

A.2.1 ESTIMATING THE LINEAR PARAMETERS

Equations of the form $\sum_i A_i X B_i = C$ for X can be solved by the iterative GMRES algorithm (Saad and Schultz, 1986) without actually computing the inverse of $\sum_i (B_i^{\top} \otimes A_i)$. So our task will be to reduce all estimates to this form.

Let $Y'_{ij} = Y_{ij} - \gamma'_{ij}$ and $\beta_i = \lambda_0 + \Lambda\alpha_i$. In order to estimate each β_i , we differentiate $\sum_j \|Y'_{ij} - S_{ij}\beta_i C_{ij}\|_F^2$ and set to 0.

$$\begin{aligned}
 & \frac{\partial}{\partial \beta_i} \sum_j \text{tr}\{(Y'_{ij} - S_{ij}\beta_i C_{ij})^\top (Y'_{ij} - S_{ij}\beta_i C_{ij})\} = 0 \\
 \implies & \sum_j \frac{\partial}{\partial \beta_i} \text{tr}\{C_{ij}^\top \beta_i^\top S_{ij}^\top S_{ij} \beta_i C_{ij}\} = 2 \sum_j \frac{\partial}{\partial \beta_i} \text{tr}\{Y_{ij}^\top S_{ij} \beta_i C_{ij}\} \\
 & \implies \sum_j C_{ij} C_{ij}^\top \beta_i^\top S_{ij}^\top S_{ij} = \sum_j C_{ij} Y_{ij}^\top S_{ij} \\
 & \implies \sum_j S_{ij}^\top S_{ij} \beta_i C_{ij} C_{ij}^\top = \sum_j S_{ij}^\top Y_{ij} C_{ij}^\top. \tag{7}
 \end{aligned}$$

This is of the form above, so we solve it to estimate each β_i , say $\hat{\beta}_i$. Then to satisfy Constraint 4 we have,

$$\hat{\lambda}_0 = \sum_i \frac{m_i \hat{\beta}_i}{\sum_i m_i}. \tag{8}$$

Now, let $\beta'_i = \hat{\beta}_i - \hat{\lambda}_0$. We know that $\beta'_i = \hat{\Lambda} \hat{\alpha}_i \hat{\xi}$. Let β denote the 3-way $b \times F \times K$ -tensor formed by stacking β'_i s. We apply the PARAFAC algorithm (Bro, 1997) for r factors on β to get the r -way canonical decomposition, denoted by $\sum_{i=1}^r w_i (\lambda_i \otimes \xi_i \otimes c_i)$, where λ_i , ξ_i and c_i are normalized. We easily get the estimates of $\hat{\lambda}$ and $\hat{\xi}^\top$ subject to Constraint (4) by stacking the λ_i s and ξ_i s respectively. Since $\hat{\alpha}_i$ s are diagonal, they can be obtained by elementwise multiplication of w_i s with c_i s, i.e.,

$$\hat{\alpha}_{i,jj} = \sum_{j=1}^r w_j c_{i,j}. \tag{9}$$

A.2.2 ESTIMATING THE VARIANCE PARAMETERS

Σ and Ψ will be estimated by the flip-flop procedure, as suggested by Glanz and Carvalho (2013). Firstly, we need an estimate of γ_{ij} . We have

$$\begin{aligned}
 & S_{ij} \gamma_{ij} C_{ij} = \gamma'_{ij} \\
 \implies & (C_{ij}^\top \otimes S_{ij}) \text{vec}(\gamma_{ij}) = \text{vec}(\gamma'_{ij}) \\
 & \implies \text{vec}(\hat{\gamma}_{ij}) = ((C_{ij}^\top \otimes S_{ij})^\top (C_{ij}^\top \otimes S_{ij}))^{-1} (C_{ij}^\top \otimes S_{ij})^\top \text{vec}(\gamma'_{ij}) \\
 & \implies \text{vec}(\hat{\gamma}_{ij}) = ((C_{ij} C_{ij}^\top) \otimes (S_{ij}^\top S_{ij}))^{-1} (C_{ij} \otimes S_{ij}^\top) \text{vec}(\gamma'_{ij}) \\
 & \implies \text{vec}(\hat{\gamma}_{ij}) = ((C_{ij} C_{ij}^\top)^{-1} \otimes (S_{ij}^\top S_{ij})^{-1}) \text{vec}(S_{ij}^\top \gamma'_{ij} C_{ij}^\top) \\
 & \implies \text{vec}(\hat{\gamma}_{ij}) = \text{vec}((S_{ij}^\top S_{ij})^{-1} S_{ij}^\top \gamma'_{ij} C_{ij}^\top (C_{ij} C_{ij}^\top)^{-1}) \\
 & \implies \hat{\gamma}_{ij} = (S_{ij}^\top S_{ij})^{-1} S_{ij}^\top \gamma'_{ij} C_{ij}^\top (C_{ij} C_{ij}^\top)^{-1}. \tag{10}
 \end{aligned}$$

Similar to Glanz and Carvalho (2013), we compute the derivatives

$$\begin{aligned}
 & \frac{\partial Q}{\partial \Sigma} = 0 \\
 \implies & -\frac{1}{2} \sum_{i,j} \left(\frac{\text{tr}\{C_{ij}^\top \Psi C_{ij}\}}{\sigma^2} S_{ij}^\top S_{ij} - \Sigma^{-1} \gamma_{ij} \Psi^{-1} \gamma_{ij}^\top \Sigma^{-1} + F_{ij} \Sigma^{-1} \right) = 0 \\
 \implies & \Sigma \left(\sum_{i,j} \frac{\text{tr}\{C_{ij}^\top \Psi C_{ij}\}}{\sigma^2} S_{ij}^\top S_{ij} \right) \Sigma + \left(\sum_{i,j} F_{ij} \right) \Sigma = \sum_{i,j} \gamma_{ij} \Psi^{-1} \gamma_{ij}^\top.
 \end{aligned}$$

Directly solving this equation will be computationally intensive, so instead, we ignore the quadratic terms and approximate Σ and Ψ by

$$\hat{\Sigma} = \sum_{i,j} \frac{\hat{\gamma}_{ij} \hat{\Psi}^{-1} \hat{\gamma}_{ij}^T}{\sum_{i,j} F_{ij}}, \quad \text{and} \quad \hat{\Psi} = \sum_{i,j} \frac{\hat{\gamma}_{ij}^T \hat{\Sigma}^{-1} \hat{\gamma}_{ij}}{\sum_{i,j} T_{ij}}. \quad (11)$$

Finally, σ^2 can be estimated as

$$\hat{\sigma}^2 = \sum_{i,j} \frac{\|Y_{ij} - S_{ij}(\hat{\lambda}_0 + \hat{\Lambda} \hat{\alpha}_i) C_{ij} - \gamma'_{ij}\|_F^2 + \text{tr}\{C_{ij}^T \hat{\Psi} C_{ij}\} \text{tr}\{S_{ij} \hat{\Sigma} S_{ij}^T\}}{\sum_{i,j} T_{ij} F_{ij}}. \quad (12)$$

After initially estimating the $\hat{\gamma}_{ij}$ values, we proceed to iteratively estimate $\hat{\Sigma}$, $\hat{\Psi}$, and $\hat{\sigma}^2$ until they reach convergence.

Appendix B. Calculations for Projection

Fix a Y , and let $\mathbf{z} = ((\xi C_Y \otimes \Lambda^T S_Y^T) M_Y^{-1} (C_Y^T \xi^T \otimes S_Y \Lambda))^{-\frac{1}{2}} \text{vec}(\hat{\alpha}_Y) = ((\xi C_Y \otimes \Lambda^T S_Y^T) M_Y^{-1} (C_Y^T \xi^T \otimes S_Y \Lambda))^{-1} (\xi C_Y \otimes \Lambda^T S_Y^T) M_Y^{-1} \text{vec}(Y - S_Y \lambda_0 \xi_Y)$, $A = (C_Y^T \xi^T \otimes S_Y \Lambda)$ and $\mathbf{x} = \text{vec}(Y - S_Y \lambda_0 C_Y)$. So $\mathbf{z} = (A^T M_Y^{-1} A)^{-1} A^T M_Y^{-1} \mathbf{x}$. Then,

$$\begin{aligned} & \|\text{vec}(Y - S_Y \lambda_0 C_Y - S_Y \Lambda \alpha_i \xi C_Y)\|_{M_Y}^2 = \|\mathbf{x} - A \text{vec}(\alpha_i)\|_{M_Y}^2 \\ & = \|\mathbf{x} - A \mathbf{z}\|_{M_Y}^2 + \|\mathbf{z} - \text{vec}(\alpha_i)\|_{A^T M_Y^{-1} A}^2 + 2\langle \mathbf{x} - A \mathbf{z}, A(\mathbf{z} - \text{vec}(\alpha_i)) \rangle_{M_Y}, \end{aligned}$$

as M_Y is symmetric positive definite. Consider only the inner product term. We have,

$$\begin{aligned} & \langle \mathbf{x} - A \mathbf{z}, A(\mathbf{z} - \text{vec}(\alpha_i)) \rangle_{M_Y} \\ & = \mathbf{x}^T M_Y^{-1} A \mathbf{z} + \mathbf{z}^T A^T M_Y^{-1} A \text{vec}(\alpha_i) - \mathbf{x}^T M_Y^{-1} A \text{vec}(\alpha_i) - \mathbf{z}^T A^T M_Y^{-1} A \mathbf{x} \\ & = \mathbf{x}^T M_Y^{-1} A (A^T M_Y^{-1} A)^{-1} A^T M_Y^{-1} \mathbf{x} + \mathbf{x}^T M_Y^{-1} A (A^T M_Y^{-1} A)^{-1} A^T M_Y^{-1} A^T M_Y^{-1} A \text{vec}(\alpha_i) \\ & \quad - \mathbf{x}^T M_Y^{-1} A \text{vec}(\alpha_i) - \mathbf{x}^T M_Y^{-1} A (A^T M_Y^{-1} A)^{-1} A^T M_Y^{-1} A (A^T M_Y^{-1} A)^{-1} A^T M_Y^{-1} \mathbf{x} \\ & = \mathbf{x}^T M_Y^{-1} A (A^T M_Y^{-1} A)^{-1} A^T M_Y^{-1} \mathbf{x} + \mathbf{x}^T M_Y^{-1} A \text{vec}(\alpha_i) \\ & \quad - \mathbf{x}^T M_Y^{-1} A \text{vec}(\alpha_i) - \mathbf{x}^T M_Y^{-1} A (A^T M_Y^{-1} A)^{-1} A^T M_Y^{-1} \mathbf{x} \\ & \implies \langle \mathbf{x} - A \mathbf{z}, A(\mathbf{z} - \text{vec}(\alpha_i)) \rangle_{M_Y} = \mathbf{0}. \end{aligned}$$

Now consider the second norm term. We have,

$$\begin{aligned} \|\mathbf{z} - \text{vec}(\alpha_i)\|_{A^T M_Y^{-1} A}^2 & = \|(A^T M_Y^{-1} A)^{-\frac{1}{2}} \text{vec}(\hat{\alpha}_Y) - \text{vec}(\alpha_i)\|_{A^T M_Y^{-1} A}^2 \\ & = \|(A^T M_Y^{-1} A)^{-\frac{1}{2}} (\text{vec}(\hat{\alpha}_Y) - (A^T M_Y^{-1} A)^{\frac{1}{2}} \text{vec}(\alpha_i))\|_{A^T M_Y^{-1} A}^2 \\ & = \|\text{vec}(\hat{\alpha}_Y) - (A^T M_Y^{-1} A)^{\frac{1}{2}} \text{vec}(\alpha_i)\|^2. \end{aligned}$$

Therefore,

$$\|\text{vec}(Y - S_Y \lambda_0 C_Y - S_Y \Lambda \alpha_i \xi C_Y)\|_{M_Y}^2 = \|\mathbf{x} - A \mathbf{z}\|_{M_Y}^2 + \|\text{vec}(\hat{\alpha}_Y) - (A^T M_Y^{-1} A)^{\frac{1}{2}} \text{vec}(\alpha_i)\|^2. \quad (13)$$

We will also compute the covariance matrix of $\text{vec}(\hat{\alpha}_Y)$

$$\begin{aligned}
 \mathbb{V}[\mathbf{x}] &= \text{cov}(\text{vec}(Y - S_Y \lambda_0 C_Y)) \\
 &= \mathbb{V}[\text{vec}(S_Y \Lambda \alpha_i \xi C_Y + S_Y \gamma C_Y + \epsilon)] \\
 &= \mathbb{V}[S_Y \gamma C_Y] + \mathbb{V}[\epsilon] \\
 &= (C_Y^\top \Psi C) \otimes (S_Y \Sigma S_Y^\top) + \sigma^2 I = M_Y \\
 \text{vec}(\hat{\alpha}_Y) &= (A^\top M_Y^{-1} A)^{-\frac{1}{2}} A^\top M_Y^{-1} \mathbf{x} \\
 \implies \mathbb{V}[\text{vec}(\hat{\alpha}_Y)] &= (A^\top M_Y^{-1} A)^{-\frac{1}{2}} A^\top M_Y^{-1} M_Y M_Y^{-1} A (A^\top M_Y^{-1} A)^{-\frac{1}{2}} \\
 &= (A^\top M_Y^{-1} A)^{-\frac{1}{2}} A^\top M_Y^{-1} A (A^\top M_Y^{-1} A)^{-\frac{1}{2}} .
 \end{aligned}$$

Thus,

$$\mathbb{V}[\text{vec}(\hat{\alpha}_Y)] = I . \quad (14)$$

Appendix C. Experimental Details

C.1 Synthetic Data set

To generate simulated data for our study, we selected $F = 2$ features, $T = 12$ time points, $K = 3$ classes, and $m_i = 100$ samples per class. A library of six functions with range $[0, 1]$ was created, and each feature-class pair was randomly assigned one function. The Σ (of dimensions $T \times T$) and Ψ (of dimensions $F \times F$) matrices were randomly generated, and they were employed to produce autoregressive noise following the matrix-variate normal distribution with a mean matrix of 0, row covariance Σ , and column covariance Ψ . Additionally, measurement errors were generated by sampling from a matrix-variate normal distribution with a mean matrix of 0 and identity covariance matrix. Samples were drawn from these matrix-variate normal distributions and added to each selected function K times to generate each sample.

To simulate missing data, for each sample, an integer T_{ij} was randomly sampled from the range of 1 to 11, representing the selected number of time points to retain. Similarly, an integer F_{ij} was randomly chosen from the range of 1 to 2, indicating the chosen number of features to retain. The T_{ij} timepoints and F_{ij} features were randomly chosen for each sample, and the rest of the data points were deleted.

C.2 The ‘‘Articulatory Word Recognition’’ Data set (Ruiz et al., 2021)

This data set comprises quite long time series, with 144 time points. We only retained every 12th time point to shorten the length while preserving the overall trend. Then, we randomly deleted some time points and some features in order to simulate the missing data. The proportion of missing time points is capped at 50% whereas it is capped at 55% for missing features.

References

- R. H. Bartels and G. W. Stewart. Algorithm 432 [C2]: Solution of the Matrix Equation $AX + XB = C$ [F4]. *Commun. ACM*, 15(9):820–826, September 1972. ISSN 0001-0782. doi: 10.1145/361573.361582. URL <https://doi.org/10.1145/361573.361582>. Place: New York, NY, USA Publisher: Association for Computing Machinery.
- Agnieszka Bier, Agnieszka Jastrzebska, and Pawel Olszewski. Variable-Length Multivariate Time Series Classification Using ROCKET: A Case Study of Incident Detection. *IEEE Access*, 10:95701–95715, 2022. ISSN 2169-3536. doi: 10.1109/ACCESS.2022.3203523. URL <https://ieeexplore.ieee.org/document/9874797/>.

- Rasmus Bro. PARAFAC. Tutorial and applications. *Chemometrics and Intelligent Laboratory Systems*, 38(2):149–171, October 1997. ISSN 0169-7439. doi: 10.1016/S0169-7439(97)00032-4. URL <https://www.sciencedirect.com/science/article/pii/S0169743997000324>.
- Hoang Anh Dau, Anthony Bagnall, Kaveh Kamgar, Chin-Chia Michael Yeh, Yan Zhu, Shaghayegh Gharghabi, Chotirat Ann Ratanamahatana, and Eamonn Keogh. The UCR time series archive. *IEEE/CAA Journal of Automatica Sinica*, 6(6):1293–1305, November 2019. ISSN 2329-9274. doi: 10.1109/JAS.2019.1911747. URL <https://ieeexplore.ieee.org/document/8894743>. Conference Name: IEEE/CAA Journal of Automatica Sinica.
- Angus Dempster, François Petitjean, and Geoffrey I. Webb. ROCKET: exceptionally fast and accurate time series classification using random convolutional kernels. *Data Min Knowl Disc*, 34(5):1454–1495, September 2020. ISSN 1573-756X. doi: 10.1007/s10618-020-00701-z. URL <https://doi.org/10.1007/s10618-020-00701-z>.
- Ronald A Fisher. The use of multiple measurements in taxonomic problems. *Annals of Eugenics*, 7(2):179–188, 1936.
- Tatsuya Fukuda, Hidetoshi Matsui, Hiroya Takada, Toshihiro Misumi, and Sadanori Konishi. Multivariate functional subspace classification for high-dimensional longitudinal data. *Jpn J Stat Data Sci*, November 2023. ISSN 2520-8764. doi: 10.1007/s42081-023-00226-x. URL <https://doi.org/10.1007/s42081-023-00226-x>.
- Sugnet Gardner-Lubbe. Linear discriminant analysis for multiple functional data analysis. *J Appl Stat*, 48(11):1917–1933, 2021. ISSN 0266-4763 1360-0532. doi: 10.1080/02664763.2020.1780569. Place: England.
- Hunter Glanz and Luis Carvalho. An Expectation-Maximization Algorithm for the Matrix Normal Distribution, September 2013. URL <http://arxiv.org/abs/1309.6609>.
- Gene Golub, Stephen Nash, and Charles Van Loan. A hessenberg-schur method for the problem $ax + xb = c$. *IEEE Transactions on Automatic Control*, 24(6):909–913, 1979.
- Ricarda Graf, Marina Zeldovich, and Sarah Friedrich. Comparing linear discriminant analysis and supervised learning algorithms for binary classification—a method comparison study. *Biometrical Journal*, 66(1):2200098, 2024.
- Alan Julian Izenman. Multivariate Regression. In Alan J. Izenman, editor, *Modern Multivariate Statistical Techniques: Regression, Classification, and Manifold Learning*, pages 159–194. Springer New York, New York, NY, 2008. ISBN 978-0-387-78189-1. doi: 10.1007/978-0-387-78189-1_6. URL https://doi.org/10.1007/978-0-387-78189-1_6.
- Gareth M. James and Trevor J. Hastie. Functional Linear Discriminant Analysis for Irregularly Sampled Curves. *Journal of the Royal Statistical Society. Series B (Statistical Methodology)*, 63(3):533–550, 2001. ISSN 13697412, 14679868. URL <http://www.jstor.org/stable/2680587>. Publisher: [Royal Statistical Society, Wiley].
- Andrew T. Jebb, Louis Tay, Wei Wang, and Qiming Huang. Time series analysis for psychological research: examining and forecasting change. *Frontiers in Psychology*, 6, 2015. ISSN 1664-1078. URL <https://www.frontiersin.org/journals/psychology/articles/10.3389/fpsyg.2015.00727>.
- Jean Kossaifi, Yannis Panagakis, Anima Anandkumar, and Maja Pantic. Tensorly: Tensor learning in python. *arXiv preprint arXiv:1610.09555*, 2016.

- Daniel Y. Lee and Jeffrey R. Harring. Handling Missing Data in Growth Mixture Models. *Journal of Educational and Behavioral Statistics*, 48(3):320–348, June 2023. ISSN 1076-9986. doi: 10.3102/10769986221149140. URL <https://doi.org/10.3102/10769986221149140>. Publisher: American Educational Research Association.
- Jason Lines, Sarah Taylor, and Anthony Bagnall. HIVE-COTE: The Hierarchical Vote Collective of Transformation-Based Ensembles for Time Series Classification. In *2016 IEEE 16th International Conference on Data Mining (ICDM)*, pages 1041–1046, December 2016. doi: 10.1109/ICDM.2016.0133. URL <https://ieeexplore.ieee.org/document/7837946>. ISSN: 2374-8486.
- Connor McLaughlin and Lili Su. Fedlda: Personalized federated learning through collaborative linear discriminant analysis. In *International Workshop on Federated Learning in the Age of Foundation Models in Conjunction with NeurIPS 2023*, 2023.
- Xiao-Li Meng and Donald B Rubin. Maximum likelihood estimation via the ecm algorithm: A general framework. *Biometrika*, 80(2):267–278, 1993.
- Matthew Middlehurst, James Large, Michael Flynn, Jason Lines, Aaron Bostrom, and Anthony Bagnall. Hive-cote 2.0: a new meta ensemble for time series classification. *Machine Learning*, 110(11-12):3211–3243, 2021.
- A. K. Gupta Nagar, D. K. *Matrix Variate Distributions*. Chapman and Hall/CRC, New York, October 1999. ISBN 978-0-203-74928-9. doi: 10.1201/9780203749289.
- Viet-Dung Nguyen, Karim Abed-Meraim, and Nguyen Linh-Trung. Fast adaptive parafac decomposition algorithm with linear complexity. In *2016 IEEE International Conference on Acoustics, Speech and Signal Processing (ICASSP)*, pages 6235–6239. IEEE, 2016.
- Paul H. C. Eilers and Brian D. Marx. Flexible Smoothing with B -splines and Penalties. *Statistical Science*, 11(2):89–102, 1996. ISSN 08834237. URL <http://www.jstor.org/stable/2246049>. Publisher: Institute of Mathematical Statistics.
- Nilam Ram and Kevin J. Grimm. Growth Mixture Modeling: A Method for Identifying Differences in Longitudinal Change Among Unobserved Groups. *Int J Behav Dev*, 33(6):565–576, 2009. ISSN 0165-0254. doi: 10.1177/0165025409343765. URL <https://www.ncbi.nlm.nih.gov/pmc/articles/PMC3718544/>.
- C Radhakrishna Rao. The utilization of multiple measurements in problems of biological classification. *Journal of the Royal Statistical Society. Series B (Methodological)*, 10(2):159–203, 1948.
- Alejandro Pasos Ruiz, Michael Flynn, James Large, Matthew Middlehurst, and Anthony Bagnall. The great multivariate time series classification bake off: a review and experimental evaluation of recent algorithmic advances. *Data Min Knowl Disc*, 35(2):401–449, March 2021. ISSN 1573-756X. doi: 10.1007/s10618-020-00727-3. URL <https://doi.org/10.1007/s10618-020-00727-3>.
- Youcef Saad and Martin H. Schultz. GMRES: A Generalized Minimal Residual Algorithm for Solving Nonsymmetric Linear Systems. *SIAM J. Sci. and Stat. Comput.*, 7(3):856–869, July 1986. ISSN 0196-5204. doi: 10.1137/0907058. URL <https://epubs.siam.org/doi/10.1137/0907058>. Publisher: Society for Industrial and Applied Mathematics.
- Yue Song, Nicu Sebe, and Wei Wang. Fast differentiable matrix square root. *arXiv preprint arXiv:2201.08663*, 2022.
- Henrik Spliid. Multivariate Time Series Estimation using marima: 38. Symposium i Anvendt Statistik 2016. *Symposium i anvendt statistik 2016*, pages 108–123, 2016. ISSN 978-87-501-2211-I. Publisher: Danmarks Statistik.

- Chang Wei Tan, Angus Dempster, Christoph Bergmeir, and Geoffrey I Webb. Multirocket: multiple pooling operators and transformations for fast and effective time series classification. *Data Mining and Knowledge Discovery*, 36(5):1623–1646, 2022.
- Pauli Virtanen, Ralf Gommers, Travis E Oliphant, Matt Haberland, Tyler Reddy, David Cournapeau, Evgeni Burovski, Pearu Peterson, Warren Weckesser, Jonathan Bright, et al. Scipy 1.0: fundamental algorithms for scientific computing in python. *Nature methods*, 17(3):261–272, 2020.
- Tingyu Wang, Simon K Layton, and Lorena A Barba. Inexact gmres iterations and relaxation strategies with fast-multipole boundary element method. *Advances in Computational Mathematics*, 48(3):32, 2022a.
- Will Ke Wang, Ina Chen, Leeor Hershkovich, Jiamu Yang, Ayush Shetty, Geetika Singh, Yihang Jiang, Aditya Kotla, Jason Zisheng Shang, Rushil Yerrabelli, Ali R. Roghanizad, Md Mobashir Hasan Shandhi, and Jessilyn Dunn. A Systematic Review of Time Series Classification Techniques Used in Biomedical Applications. *Sensors*, 22(20):8016, January 2022b. ISSN 1424-8220. doi: 10.3390/s22208016. URL <https://www.mdpi.com/1424-8220/22/20/8016>. Number: 20 Publisher: Multidisciplinary Digital Publishing Institute.
- Fang Yao, Hans-Georg Müller, and Jane-Ling Wang. Functional Data Analysis for Sparse Longitudinal Data. *Journal of the American Statistical Association*, 100(470):577–590, 2005. ISSN 01621459. URL <http://www.jstor.org/stable/27590579>. Publisher: [American Statistical Association, Taylor & Francis, Ltd.].
- Jinsung Yoon, William R. Zame, and Mihaela van der Schaar. Estimating Missing Data in Temporal Data Streams Using Multi-Directional Recurrent Neural Networks. *IEEE Transactions on Biomedical Engineering*, 66(5):1477–1490, May 2019. ISSN 1558-2531. doi: 10.1109/TBME.2018.2874712. URL <https://ieeexplore.ieee.org/document/8485748>. Conference Name: IEEE Transactions on Biomedical Engineering.
- Fa Zhu, Junbin Gao, Jian Yang, and Ning Ye. Neighborhood linear discriminant analysis. *Pattern Recognition*, 123:108422, 2022.